Role of the Coordinating Histidine in Altering the Mixed Valency of Cu_A: An Electron Nuclear Double Resonance-Electron Paramagnetic Resonance Investigation

Dmitriy Lukoyanov,* Steven M. Berry,† Yi Lu,† William E. Antholine,‡ and Charles P. Scholes*

*Department of Chemistry and Center for Biological Macromolecules, University at Albany, SUNY, Albany, New York 12222 USA;
†Department of Chemistry, Chemical & Life Sciences Laboratory, University of Illinois, Urbana, Illinois 61801 USA; and
‡National Biomedical Electron Spin Resonance Center, Biophysics Research Institute, Medical College of Wisconsin, Milwaukee, Wisconsin 53226 USA

ABSTRACT The binuclear Cu_A site engineered into *Pseudomonas aeruginosa* azurin has provided a Cu_A-azurin with a well-defined crystal structure and a CuSSCu core having two equatorial histidine ligands, His120 and His46. The mutations His120Asn and His120Gly were made at the equatorial His120 ligand to understand the histidine-related modulation to Cu_A, notably to the valence delocalization over the CuSSCu core. For these His120 mutants Q-band electron nuclear double resonance (ENDOR) and multifrequency electron paramagnetic resonance (EPR) (X, C, and S-band), all carried out under comparable cryogenic conditions, have provided markedly different electronic measures of the mutation-induced change. Q-band ENDOR of cysteine C_β protons, of weakly dipolar-coupled protons, and of the remaining His46 nitrogen ligand provided hyperfine couplings that were like those of other binuclear mixed-valence Cu_A systems and were essentially unperturbed by the mutation at His120. The ENDOR findings imply that the Cu_A core electronic structure remains unchanged by the His120 mutation. On the other hand, multifrequency EPR indicated that the H120N and H120G mutations had changed the EPR hyperfine signature from a 7-line to a 4-line pattern, consistent with trapped-valence, Type 1 mononuclear copper. The multifrequency EPR data imply that the electron spin had become localized on one copper by the His120 mutation. To reconcile the EPR and ENDOR findings for the His120 mutants requires that either: if valence localization to one copper has occurred, the spin density on the cysteine sulfurs and the remaining histidine (His46) must remain as it was for a delocalized binuclear Cu_A center, or if valence delocalization persists, the hyperfine coupling for one copper must markedly diminish while the overall spin distribution on the CuSSCu core is preserved.

INTRODUCTION

Cu_A in cytochrome *c* oxidase was recognized even in the 1970s as having unusual electronic properties (Beinert, 1997), for example, by its small histidine and Cys C_β proton hyperfine couplings (Stevens et al., 1982; van Camp et al., 1978) and by its small copper hyperfine couplings resolved at S-band (Froncisz et al., 1979). Subsequently, the marked similarities between the Cu_A center of cytochrome oxidase and the binuclear copper of nitrous oxide reductase in their low frequency, seven-line EPR pattern (Antholine, 1997; Karpefors et al., 1996; Kroneck et al., 1990) and in the considerable homology of sequence near the copper binding sites (Zumft et al., 1992; Zumft and Kroneck, 1996) all pointed to Cu_A as a binuclear, mixed-valence [Cu(1.5)···Cu(1.5)] center. Mixed-valency will arise when there is a large exchange coupling that delocalizes an unpaired valence electron throughout the CuSSCu core and when this coupling is larger than vibronic, Jahn-Teller-like interactions or any local copper site differences that tend to valence-trap spin on one of the coppers (Farrar et al., 1996; Schatz, 1980). The purple Cu_A center was firmly established as a binuclear, mixed-valence complex through biophysical (Blackburn et al., 1994; Farrar et al., 1995; Greenwood et al., 1983; Kroneck et al., 1990), biochemical (Dennison et al., 1995; Hay et al., 1996; Slutter et al., 1996; van der Oost et al., 1992), and x-ray crystallographic study (Iwata et al., 1995; Robinson et al., 1999; Tsukihara et al., 1995; Williams et al., 1999; Wilmanns et al., 1995). The Cu_A center (called Cu_A-azurin hereafter) as engineered by loop-directed mutagenesis into *Pseudomonas aeruginosa* azurin (Hay et al., 1996, 1998) provided high resolution (1.65 Å) to the structure of Cu_A in a protein, whereby bond distances to weaker axial ligands and to equatorial histidine ligands were obtained along with the tilt of the histidine imidazole planes. (A schematic of the locale of the Cu_A centers from wild-type Cu_A-azurin is shown in Fig. 1.) One histidine ligand (His120/H120) conspicuously showed both a longer bond distance and a larger out-of-plane tilt than the other histidine (His46/H46), and the copper that coordinated His120 also happened to be the recipient of a short bond to a carbonyl oxygen, whose Cu-oxygen bond length was little different from the His120-to-Cu bond distance. The existence of two detectable and structurally slightly different Cu_A centers within the wild-type Cu_A-azurin crystal with different Cu-His120 bond lengths was resolved, as indicated in

Submitted November 17, 2001, and accepted for publication February 13, 2002.

Dr. Lukoyanov is on leave from the MRS Laboratory, Kazan State University, 420008, Kazan, Russian Federation.

Address reprint requests to Dr. Charles P. Scholes, Department of Chemistry, University at Albany, SUNY, Albany, NY 12222. Tel: 518-442-4551; Fax: 518-442-3462; E-mail: cps14@ albany.edu.

0006-3495/02/05/2758/09 $2.00

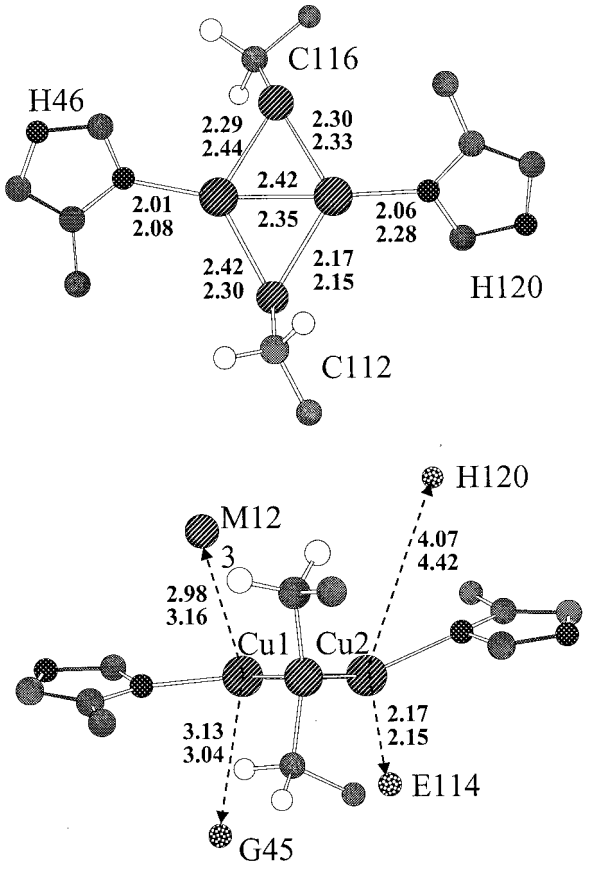

FIGURE 1 This schematic shows a top view (*top schematic*) and side view (*bottom schematic*) of the local environs (Robinson et al., 1999) of the Cu_A center in Cu_A-azurin. Because two slightly different Cu_A sites were revealed (Robinson et al., 1999) from the crystal structure, the distances in Å in the top and bottom rows are for the two sites. The directly coordinating Cys116, Cys112, His46, and His120 side chains are shown; the light atoms on C112 and C116 are the Cys C_β protons. The nearest atoms of weak axial ligands are also shown, and these are sulfur of Met123 and the carbonyl oxygens of E114, H120, and G45.

Fig. 1. Wild-type Cu_A-azurin showed the typical 7-line EPR pattern characteristic of mixed-valence [Cu(1.5)···Cu(1.5)] copper (Hay et al., 1998).

As observed from crystal structures of recombinant and native Cu_A systems (Iwata et al., 1995; Tsukihara et al., 1995; Wilmanns et al., 1995; Robinson et al., 1999), the axial ligand distance, Cu-Cu bond distance, and equatorial histidine nitrogen bonding are interdependent (Farrar et al., 1996, Gamelin et al., 1998). Furthermore, they are coupled to the electron transfer function of the site by their affect on the reduction potential, bonding, reorganization energy, and electronic structure of the copper center. In an effort to modulate the bonding of the equatorial ligand, and thus vary the axial ligand interaction and Cu-Cu bonding, His120 was mutated to asparagine and glycine in Cu_A azurin (Wang et al., 1999; Berry et al., 2000).

ENDOR-EPR measurements are relevant to this biological electron transfer function and bonding because they provide an experimental measure of electron delocalization and an experimental measure of unpaired spin density on the cysteine and histidine ligands through which electron transfer may occur. Multifrequency EPR and Q-band ENDOR studies were done to identify the underlying electronic structural character of Cu_A-azurin and its His120 mutants and to identify the role of His120 in altering this electronic structural character (Berry et al., 2000; Wang et al., 1999).

MATERIALS AND METHODS

The Cu_A-azurin, its His120Asn (H120N) and His120Gly (H120G) mutants, and Type 1 azurin per se were expressed, prepared, and characterized as described previously (Hay et al., 1996; Wang et al., 1999). The concentration of these samples was ~1 mM, and they were dissolved in 50% glycerol, 0.1 M phosphate buffer, pH 5.2. Beef heart cytochrome *c* (aa_3) oxidase was prepared as described previously (Fan et al., 1988). Copper-substituted liver alcohol dehydrogenase in the presence of NADH (Maret and Kozlowski, 1987) was prepared by C. T. Martin. ENDOR experiments were carried out at Q-band (Sienkiewicz et al., 1996) under cryogenic, pumped helium rapid passage conditions as outlined previously (Veselov et al., 1998). Cryogenic multifrequency EPR spectra at S, C, and X-band were taken and analyzed at the National Biomedical ESR Center (Antholine, 1997). Loop-gap resonators and low frequency microwave bridges designed and built at the National Biomedical ESR Center (Medical College of Wisconsin, WI) were used at S- and C-band (Froncisz and Hyde, 1982). The temperature for multifrequency EPR was controlled with a helium flow system (Air Products, Allentown, PA). A Gaussmeter (Rawson-Lush Instrument, Inc., Acton, MA) was used to calibrate the magnetic field and an EIP Model 548 frequency counter used to measure the microwave frequency.

RESULTS

Multifrequency EPR

The EPR results for Cu_A-azurin at X-band (9.2 GHz), C-band (4.5 GHz), and S-band (3.4 GHz) in Fig. 2 *A* showed a seven-line pattern aligned on a common $g_\parallel = 2.17$ with relative intensities 1:2:3:4:3:2:1 characteristic of a single electron delocalized over two equivalent coppers. The copper hyperfine coupling was 56 Gauss near $g_\parallel$ and 38 Gauss near $g_\perp$. The corresponding spectra from the mutants H120N and H120G showed overall less detail, but there was a feature centering at $g_\parallel = 2.23$ at all EPR frequencies with resolved splittings of ~40 G. For H120N the copper hyperfine structure in the $g_\parallel$ region was well defined at C-band (4.45 GHz) where three of four hyperfine lines were resolved (Fig. 2 *B*). At S-band (3.38 GHz), two hyperfine lines in the $g_\parallel$ region were resolved, but the third and fourth lines were superimposed with the $g_\perp$ region. At X-band, three lines were resolved in the $g_\parallel$ region, but the fourth line was broadened and the third line did not line up as well with the spectra at low frequencies (Fig. 2 *B*), possibly due to second-order shifts. Besides the constant $g_\parallel$ values determined from the H120N mutants for these three frequencies, where $g = 2.23$ is consistent with $g_\parallel$ for a mononuclear

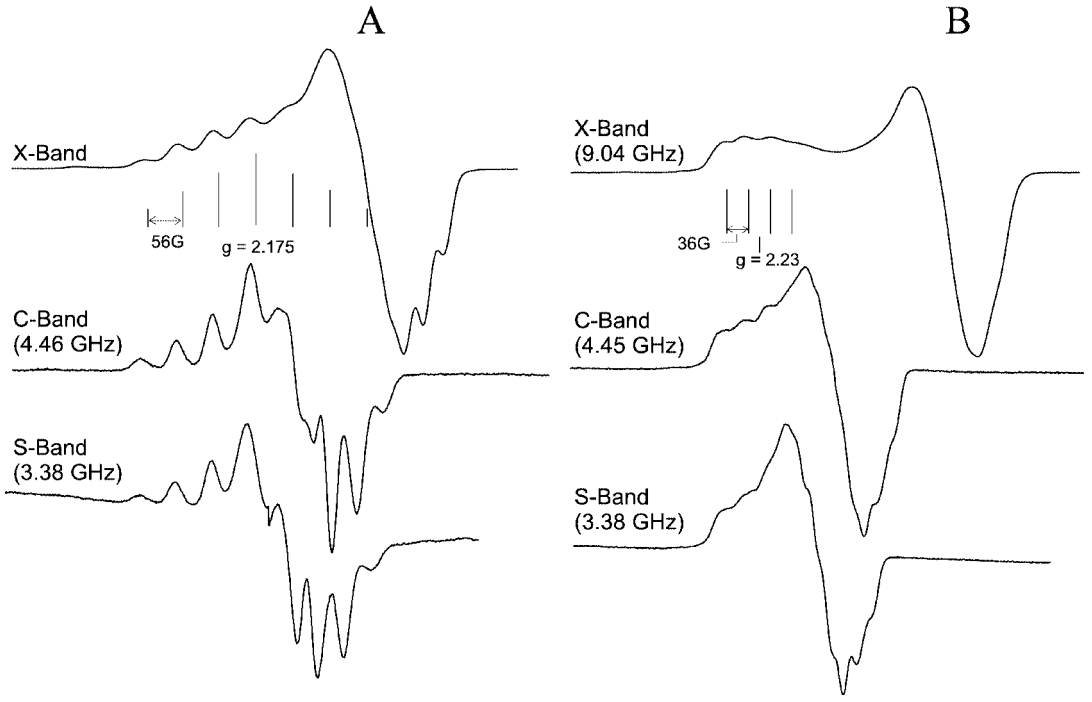

FIGURE 2 This figure provides a comparison of S-band, C-band, and X-band spectra of Cu_A-azurin (*A*) and H120N (*B*). Experimental conditions: temperature 15 K; microwave power 23 dB down from an incident power of 7 mW, time constant 0.1 s; scan time 4 min; modulation amplitude 5 G; gain 3.2×10^2; cavity, loop-gap resonator at S and C band. Standard TE102 resonator was used at X-band with 5 mW power.

copper site (Solomon et al., 1992), there was a well-defined edge to the low field side of the $g_\parallel$ region. Such a well-defined edge supports a four-line mononuclear copper pattern with intensity ratios of 1:1:1:1 rather than the broader seven-line pattern with intensity ratios of 1:2:3:4:3:2:1. Overall, the combined wild-type Cu_A-azurin X, C, and S-band EPR spectra were interpreted in terms of a seven-line pattern centered at $g_\parallel = 2.17$ (seven evenly spaced vertical lines with relative intensity 1:2:3:4:3:2:1 in Fig. 2) and for the combined X, C, and S-band spectra of the His120 mutants in terms of a four-line pattern centered at $g_\parallel = 2.23$ (see four evenly spaced vertical lines with the same relative intensity in Fig. 2, also Table 1).

Rapid passage Q-band (34.1 GHz) EPR signals (Fig. 3 *a*) taken in the course of ENDOR study, whose shape appears as an absorption line shape, also gave an apparent value of $g_\parallel = 2.17$ for Cu_A-azurin and $g_\parallel = 2.22$ for its H120N and H120G mutants. For H120G, which is the least stable of the mutants, the Q-band rapid passage signal showed evidence for a minority component of Type 2 copper with $g_\parallel > 2.3$. Fig. 3 *b* shows the numerically determined first derivative signals of Cu_A-azurin and H120N. For H120N the *g* tensor was essentially axial with $g_\perp = 2.007$; if there was any unresolved $g_x - g_y$ anisotropy, it was no more than 0.005 *g* value units. For wild-type Cu_A-azurin $g_\perp = 2.018$.

Proton ENDOR

Proton ENDOR frequencies, ${}^P\nu_{ENDOR}$, center to first order at the proton Larmor frequency, ν_P (> 44 MHz for fields used at Q-band) and split away from the proton Larmor

TABLE 1 Multifrequency EPR findings

Sample	$g_z^{Cu\text{-}Cu}$*	g_z^{Cu}†	A_z‡§	ν_e (GHz)
Wild type				
S-Cu_A	2.18	2.36	58G	3.38
C-Cu_A	2.17	2.31	55G	4.46
X-Cu_A	2.18	2.24	56G	9.06
Mutants				
S-H120G	2.13	2.23	34G	3.38
S-H120N	2.12	2.23	36G	3.38
C-H120G	2.15	2.24	36G	4.45
C-H120N	2.15	2.23	36G	4.45
X-H120G	2.18	2.24	40G	9.08
X-H120N	2.19	2.24	40G	9.05

*$g_z^{Cu\text{-}Cu}$ was calculated assuming a seven-line pattern beginning with the first resolved line in the $g_\parallel$ region.

†g_z^{Cu} was calculated assuming a four-line pattern, also beginning with the first resolved line on the low field side in the $g_\parallel$ region.

‡The error in A_z is ±4 G, determined from the average of different spectra taken on different spectrometers.

§An unusual feature of the lines in the $g_\parallel$ region is broadening of the high field line in the $g_\parallel$ region. This is attributed to *g*-strain and *A*-strain and is a reason why it is difficult to distinguish between a seven-line pattern and a four-line pattern at a single frequency.

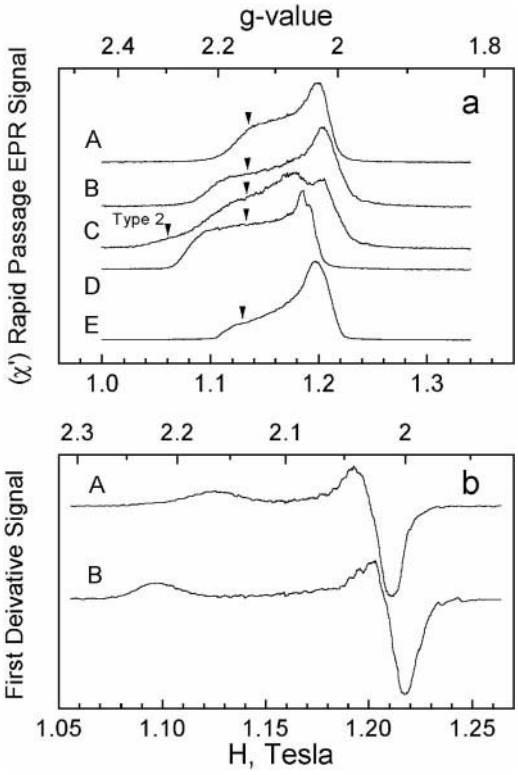

FIGURE 3 (*a*) The Q-band rapid passage EPR spectra taken at 1.9 K under adiabatic rapid passage conditions similar to those used for ENDOR. We compare Cu_A-azurin (*A*), H120N (*B*) and H120G (*C*) mutants, and monocopper azurin (*D*), and monocopper CuLADH (*E*). Arrow indicates where we took the comparison ENDOR spectra in Figs. 4, 5, and 6 in the text. We note that there is a low field (high *g* value) Type 2 feature from H120G. (For these spectra $T = 1.9$ K, 5 scans $\times$ 21 s, modulation = 2 G, $\nu_e = 34.09$ GHz, 0.24-μW microwave power.) (*b*) Comparison of the numerical first derivative spectra of the above rapid passage Cu_A-azurin (*A*) and H120N (*B*) signals. *g* values as well as magnetic field strength are provided on the horizontal axis.

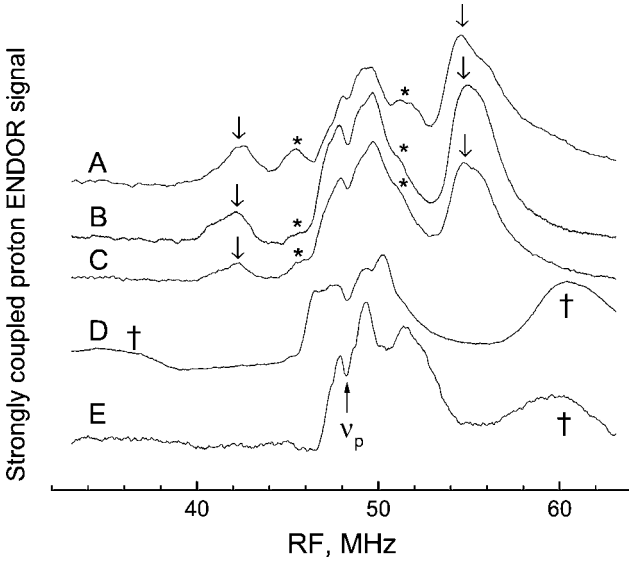

FIGURE 4 This figure compares the strongly coupled proton ENDOR spectra that show features that we assign as the Cys C_β protons of Cu_A-azurin (*A*), the H120N mutant (*B*), the H120G mutant (*C*), monocopper azurin (*D*), and monocopper CuLADH (E). The features with arrows have coupling of ~13 MHz, and the features with stars have coupling of ~6 MHz. The monocopper azurin and CuLADH both show much larger couplings (24 MHz, *daggers*) than found with Cu_A systems. (Conditions were microwave power = 0.24 μW, modulation 2.4 G, RF power ~20 W pulsed, $\nu_e = 34.09$ GHz, $H = 1.128$ T, $g = 2.16$. Frequency sweep rate 3 MHz/s, and each spectrum was the average of 15 traces, each taking 10 s.)

frequency by $\pm 1/2A$, in which A is the hyperfine coupling. Thus, the ENDOR frequencies are ${}^{P}\nu_{ENDOR}{}^{\pm} = /\nu_p \pm A/2/$ (Hoffman et al., 1993; Veselov et al., 1998; Werst et al., 1991). Under rapid passage conditions the intensity of the two branches need not be the same (Hoffman et al., 1993; Veselov et al., 1998; Werst et al., 1991). At Q-band the proton ENDOR near 50 MHz is well separated from nitrogen ENDOR below 30 MHz. We show in Fig. 4, *A* to *C*, similar, strongly coupled proton features (arrows) measured at $g = 2.16$ from wild-type Cu_A-azurin and its H120N and H120G mutants, respectively, having couplings of $A = 12.1 \pm 0.2$, 12.8 ± 0.2, and 12.4 ± 0.2 MHz. Such couplings are of the order previously observed for Cys C_β features (Gurbiel et al., 1993; Neese et al., 1998; Stevens et al., 1982; van Camp et al., 1978), and a compendium of ENDOR spectra (provided for reviewers) taken over a range of *g* values from 2.23 to 2.01 showed their isotropic nature. There were also smaller proton couplings, respectively, of 5.7 ± 0.2, 5.5 ± 0.3, and 5.3 ± 0.3 MHz (starred), somewhat better resolved and of slightly higher frequency in wild-type Cu_A-azurin but appearing as shoulders in the H120N and H120G mutants. If the electron on a mutant Cu_A were to exhibit trapped valence behavior, its locale would include cysteine and histidine ligands as are found in Type 1 copper. Therefore, we show in Fig. 4 *D* the considerably larger Cys C_β proton couplings (with daggers) that arise from mononuclear Type 1 copper (azurin) having one cysteine ligand and two histidines, and in Fig. 4 *E* is shown the proton coupling arising from mononuclear CuLADH whose copper has two cysteine ligands and one histidine (Maret and Kozlowski, 1987; Ramaswamy et al., 1996). In both cases the proton couplings, which are from Cys C_β protons, are much larger than even the largest found from Cu_A-azurin or its H120N or H120G histidine mutants. It would be difficult to mistake the Cys C_β proton of valence-delocalized Cu_A for the Cys C_β proton of monocopper type copper.

There is a range of weak proton couplings within approximately ± 2 MHz of ν_P, which largely reflect dipolar couplings with inverse cube distance dependence to the nearest metal (Neese et al., 1998), and these showed very similar features for both Cu_A-azurin and its H120N and H120G mutants (Fig. 5, *A–C*). Mononuclear azurin, however, had a considerably larger spread to its weakly coupled proton ENDOR (Fig. 5 *D*); whereas for CuLADH the spread was less than for the Cu_A systems (Fig. 5 *E*).

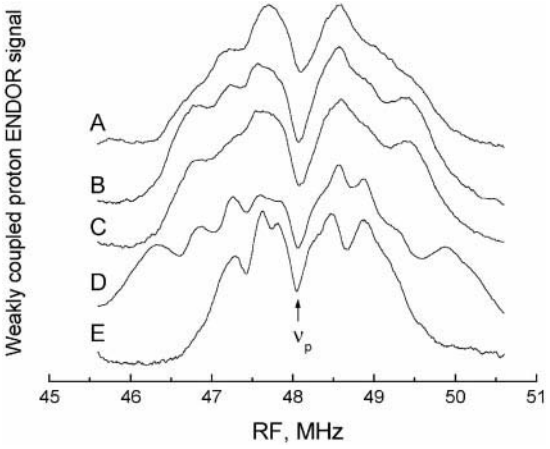

FIGURE 5 The purpose of this figure is to compare weakly coupled proton features from Cu_A-azurin (*A*), the H120N (*B*) and H120G (*C*) mutants, azurin (*D*), and CuLADH (*E*). We make no assignments at this time, other than to point out that such weak couplings are typically dipolar from noncovalently linked protons. The similarity of the spectra of Cu_A-azurin, H120N, and H120G indicates a similar overall CuSSCu core spin density distribution for these three systems. (Conditions were 0.24-μW microwave power, 100-KHz modulation = 0.5 G, RF power ~20 W pulsed with 10% duty cycle, ν_e = 34.09 GHz, H = 1.128 T, T = 1.9 K. Frequency sweep rate 0.5 MHz/s, and each spectrum was the average of ~40 traces.)

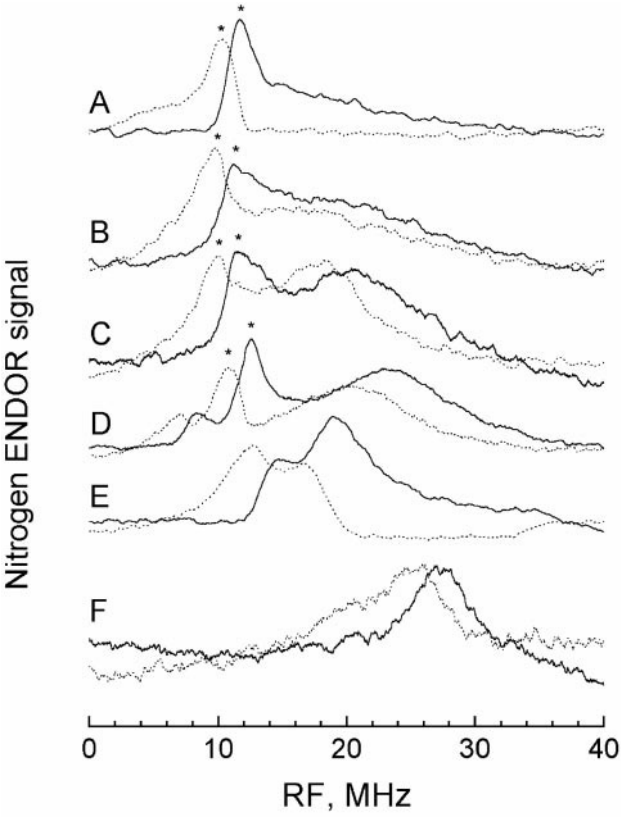

FIGURE 6 This figure compares the ^{14}N ENDOR nitrogen spectra in the region of 0 to 40 MHz from Cu_A-azurin (*A*), from the H120N mutant (*B*), from the H120G mutant (*C*), from Cu_A of beef heart cytochrome *c* oxidase (*D*), Type 1 azurin (*E*), and CuLADH (*F*). The starred feature is characteristic of Cu_A nitrogen. The purpose of showing frequency sweeps from low-to-high (*solid line*) and high-to-low (*dashed line*) is to distinguish the relaxation tail of various features, which occurs in the direction of the sweep because the peaks will be shifted in the direction of the sweep by spin relaxation and by the experimental time constant. (Conditions were: T = 1.9 K, 7.8-nW microwave power, 2-G modulation, 20-W RF power, pulsed with 10% duty cycle, ν_e = 34.09 GHz, H = 1.128 T. Frequency sweep rate 4 MHz/s, and each spectrum was the average of ~250 traces, each taking 10 s.)

Nitrogen ENDOR

Histidine nitrogen ENDOR for both Cu_A and Type 1 systems occurs in the 1 to 30 MHz region. The first-order expressions for ^{14}N ENDOR frequencies are: $^{14}\nu_{ENDOR}{}^{+} = /A/2 \pm 3/2P + {}^{14}\nu/$ and $^{14}\nu_{ENDOR}{}^{-} = /A/2 \pm 3/2P - {}^{14}\nu/$, in which A is the hyperfine coupling, P the quadrupolar coupling, and $^{14}\nu$ (3.7 MHz at 1.20 T) is the ^{14}N nuclear Zeeman frequency. Particularly with Q-band rapid passage ENDOR, the $^{14}\nu_{ENDOR}{}^{+}$ branch is often the only branch observed for ^{14}N (Hoffman et al., 1993; Veselov et al., 1998; Werst et al., 1991). For Cu-histidine ligation the ^{14}N hyperfine interaction is generally dominated by isotropic Fermi coupling due to unpaired electron spin density in the nitrogen 2-s orbital, and the elements of the quadrupolar tensor have typical magnitudes $/P/ \leq 1.1$ MHz (McDowell et al., 1989). Cu_A-azurin, its H120N and H120G mutants, and Cu_A of beef heart cytochrome *c* oxidase all showed a feature (starred in Fig. 6) near 11 MHz, and the ^{14}N hyperfine couplings (A) of this feature, as taken at the common g value of 2.16, were estimated at 15.1, 14.1, 14.5, and 16.7 ($\pm$ 0.3) MHz. Noting the caveat that ENDOR is a double resonance technique not ideal for counting nuclear spins, we point out that the ratio of the peak height of the ^{14}N feature to the central proton features near ν_p was twice as large for wild-type Cu_A-azurin as for H120N; this doubled ratio is consistent with the existence of two histidine ligands with identical couplings for wild-type Cu_A-azurin but only one histidine ligand for the His120 mutant. The rapid passage nitrogen features of all Cu_A samples showed a relaxation "tail" extending in the direction of the frequency sweep, and to properly resolve the relevant nitrogen features in the wide 40-MHz frequency sweep of Fig. 6, we provide spectra with frequency sweeps from both low-to-high (solid line) and high-to-low (dashed line) directions. In addition to ^{14}N features we and others, (P. Doan, personal communication) who use rapid passage methods for Q-band ENDOR, have consistently noted in all Cu_A samples, including these samples, various cytochrome *c* oxidases, and nitrous oxide reductase, a broad peak in the 20- to 30-MHz range, and we and others assign it to the ν^- branch of $^{63,65}Cu$ ENDOR. (Expressions for the ENDOR frequencies of the $\nu^{\pm}$ branches of $^{63,65}Cu$ are given by Gurbiel et al. (1993) in terms of one-half the copper hyperfine coupling, the copper quadrupolar coupling, and the copper nuclear Zeeman in-

teraction, in which the latter is ~13 MHz at 1.13 T. For the ν^- branch the copper nuclear Zeeman interaction provides a negative contribution of −13 MHz so that features belonging to the ν^- branch will occur below one-half the copper hyperfine coupling in a frequency range below 50 MHz.) ^{14}N spectra (provided for reviewers) taken over a range of g values from 2.23 to 2.01 showed additional splittings to the ^{14}N features in the $g_\perp$ (2.03–2.004) region similar to those previously noted from cytochrome *c* oxidases (Gurbiel et al., 1993) and assigned to anisotropy in hyperfine and quadrupole couplings.

If the unpaired electron of a His120 mutant were to exhibit trapped valence behavior at the copper ligated to His46, the resultant center could well exhibit ^{14}N histidine hyperfine couplings similar to those of monocopper Type 1 azurin or CuLADH, whose nitrogen ENDOR spectra we therefore show. The Type 1 azurin sample (Fig. 6 *E*) had two nitrogen ENDOR features located at average frequencies of 13.5 ± 1 and 17.5 ± 1 MHz; these signals corresponded to couplings of 20 and 28 MHz, consistent with those reported by Werst et al. (1991). There were nitrogen signals from CuLADH (Fig. 6 *F*), which appeared near 25 MHz with ^{14}N couplings >40 MHz. For both monocopper azurin and CuLADH the larger ^{14}N ENDOR frequencies were highly unlike those resolved from all of our Cu_A systems.

ENDOR from Type 2 copper in H120G

For H120G, there was also an additional impurity signal observable by Q-band rapid passage EPR as a low field shoulder in Fig. 2 *A*, and we were able to characterize it (Fig. 7) as a Type 2 copper signal lacking cysteine but having nitrogenous ligands. The minority Type 2 features from the H120G mutant do not interfere with the resolution of the ^{14}N histidine or the strong Cys C_β proton couplings belonging to the Cu_A center in this mutant. At the high g value of 2.30 and field of 1.058 *T*, where Type 2 copper solely occurs, we obtained a nitrogen ENDOR spectrum similar to the Type 2 nitrogen spectrum (Fig. 7 *a*) observed in nitrite reductase near 20 MHz (Veselov et al., 1998), and we obtained from H120G a proton spectrum (Fig. 7 *b*), which showed no strongly coupled Cys C_β protons but only protons with hyperfine couplings less than 6 MHz.

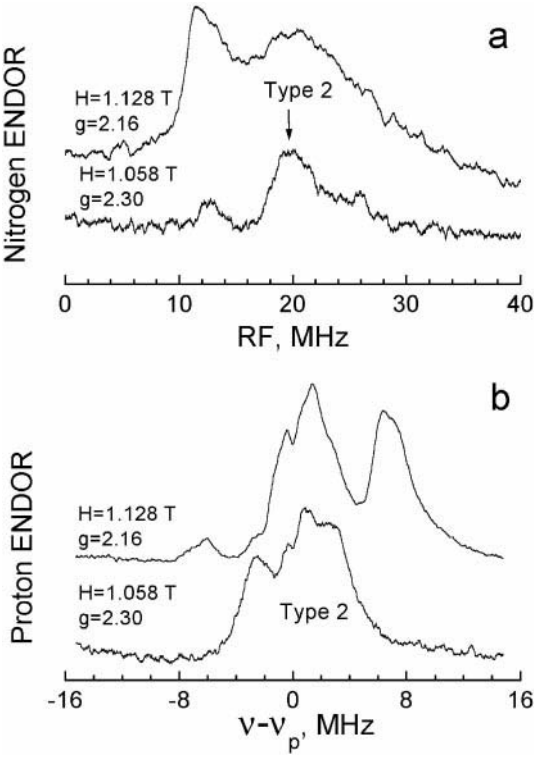

FIGURE 7 Purpose of this figure is to demonstrate that H120G contains a Type 2 copper lacking a cysteine ligand but having nitrogen ligands. (*a*) Compares the nitrogen spectrum at a field of 1.058 T (g = 2.30), where there is only Type 2 copper with that at H = 1.128 T (g = 2.16) in which both Cu_A and Type 2 copper occur; this comparison demonstrates that the feature near 20 MHz is from Type 2 copper. (*b*) Compares the proton spectrum at a field of 1.058 T (g = 2.30), which lacks couplings larger than 6 MHz with the proton spectrum at the field of 1.058 T where larger couplings from the β-cysteine protons of Cu_A occur.

DISCUSSION

Q-band ENDOR

The ~12- to 14-MHz Cys C_β proton couplings observed and measured in detail in Fig. 4 for wild-type Cu_A-azurin and its H120N and H120G mutants were compatible with Cys C_β proton frequencies seen from other Cu_A complexes (e.g., A = 12, 19 MHz from Cu_A in beef heart oxidase (Gurbiel et al., 1993; Stevens et al., 1982; van Camp et al., 1978; Werst et al., 1991), or A = 8.6, 10.4, 11.7, and 13.3 MHz from Cu_A in nitrous oxide reductase (Neese et al., 1998)). The Type 1 azurin with one cysteine ligand and the CuLADH having two cysteine ligands are mononuclear Type 1 systems having considerably larger Cys C_β proton couplings, consistent with those reported by Werst et al. (1991), than does Cu_A. At ambient temperature (278 K), a Fermi contact term of 12.5 MHz would translate into a proton contact shift of 355 ppm, which compares favorably with the 300 to 500 ppm contact shifts for Cys C_β protons measured by nuclear magnetic resonance of Cu_A from *Paracoccus denitrificans* (Luchinat et al., 1997). The Cys C_β proton hyperfine coupling arises by a hyperconjugative mechanism (Atherton, 1973) that depends on the spin population in the adjacent π orbital on the sulfur and on the relative orientation of the C_β-H_β bond and the spin containing π orbital on the adjacent sulfur (Gurbiel et al., 1993; Neese et al., 1998; Werst et al., 1991). The reason for the much larger Cys C_β couplings of monocopper azurin and CuLADH is that the cysteine in these cases has a larger spin density than an individual cysteine of Cu_A-azurin. The Cys

C_β proton ENDOR provides information on the spin density in the adjacent sulfur π orbitals and on the conformation of the cysteine. If the Cys C_β proton ENDOR signals do not change in going from wild-type Cu_A-azurin to the H120N and -G mutants of Cu_A-azurin, then the spin population on the cysteine and the conformation of the cysteine do not change.

Weak proton couplings will arise from dipolar interactions, which are dependent on spin density on the copper or sulfur center near the proton of interest and on the inverse cube of the distance to that spin density (Hoffman et al., 1993; Veselov et al., 1998). The similarity of the ENDOR pattern from weakly coupled protons was a qualitative but strong indicator that the general distribution of unpaired electron spins throughout the CuSSCu core was unchanged between Cu_A-azurin and its H120N and H120G mutants. Mononuclear azurin, however, had a considerably larger spread in its weakly coupled proton ENDOR, perhaps reflecting localization of greater spin density on its one copper, whereas the spread of weak couplings was less for the CuLADH, possibly due to delocalization of spin to its two sulfurs.

The nitrogen hyperfine couplings, both for wild-type Cu_A-azurin and for its His120N and -G mutants, were similar to each other and to those observed for previously studied Cu_A (Gurbiel et al., 1993; Neese et al., 1998), and these couplings were not the larger ^{14}N couplings to mononuclear Type 1 systems. Evidently, the histidine ^{14}N hyperfine couplings of His120 and His46 were quite similar to each other in wild-type Cu_A-azurin, and the loss of His120 did not substantially change the ^{14}N hyperfine coupling to the remaining His46. The histidine nitrogen coupling largely depends on unpaired electron spin density in the nitrogen 2-s orbital, where that spin density arises there from sigma bonding overlap with copper orbitals. The H120N and H120G mutants of Cu_A-azurin have lost one nitrogen but have retained the same nitrogen coupling as previously to the other His46 nitrogen. If there is little change in the nitrogen hyperfine coupling, the implication is that there is little change in the spin density on the adjacent copper.

Multifrequency EPR

The most obvious spectroscopic perturbation from the H120N and H120G mutations is in their multifrequency EPR hyperfine spectrum, which is changed from a 7-line spectrum typical of a mixed-valence binuclear center to a spectrum with at most four lines, which is more typical of valence-trapped Type 1 copper. Trapping the valence on one copper is the most obvious way of eliminating the hyperfine coupling and *g*-value contribution from the other copper. The $g_\parallel$ value of the His120 mutants is more consistent with a mononuclear Type 1 copper (Antholine, 1997; Neese, 1997). An $A_\parallel$ value of 40 G from the spectra of the His120 mutants is on the low side of the expected $A_\parallel$ value for a Type 1 copper. If the mutated site in Cu_A-azurin were valence trapped, the expected value for $A_\parallel$ would be 112 G (56 G $\times$ 2) (Neese et al., 1996), but the resolved coupling is one-half of this.

Whether an individual copper is valence-trapped or part of a valence-delocalized system, the relation of copper *g* values and copper hyperfine coupling to the electronic structure and spin population on the copper is complex (Maki and McGarvey, 1958; Neese, 1997). The difference of *g* values from 2.00 depends on spin orbit coupling of the ground state to excited *d* electron levels. The copper hyperfine coupling depends in a complex fashion on Fermi hyperfine coupling to metal *s* electrons, on dipolar nuclear hyperfine coupling to metal electron spin, and on nuclear hyperfine coupling to unquenched metal orbital angular momentum. These hyperfine contributions may be of opposite sign so that in principal it would be possible to maintain the same spin density on a copper but to have a different blend of these contributions that would yield components of the copper hyperfine tensor close to zero. Whether the mix of copper electronic orbitals necessary to achieve such a zero hyperfine tensor would properly lend itself to the electronic overlap and to the set of electronic configurations necessary for valence delocalization (Neese, 1997) is problematic.

CONCLUSION

The wild-type Cu_A-azurin system, although engineered into a Type 1 copper azurin through loop-directed mutagenesis, showed intimate electronic structure and hyperfine information from its cysteines, histidine, and copper, which are highly typical of the Cu_A of naturally occurring systems. The characteristics of the Cys C_β proton and histidine hyperfine couplings that reflected specific covalency of the CuSSCu core, as well as the weak proton couplings that qualitatively reflected overall spin distribution, remained essentially unchanged among Cu_A-azurin and its H120N and H120G mutants. The ENDOR findings and UV-Vis (Berry et al., 2000; Wang et al., 1999) information would imply that the core electronic structure remains unchanged among Cu_A-azurin and its H120N and H120G mutants. Multifrequency EPR at similar cryogenic temperatures to those of ENDOR showed that the His120 mutations led to an increase in $g_\parallel$ (2.17–2.23) and a copper hyperfine pattern that diminished from the seven lines expected from mixed-valence copper to no more than four copper features in a manner that might be expected from trapped-valence mononuclear copper. These results indicate that the His120 ligand plays a subtle role in modulation of electronic structure of the Cu_A center and different spectroscopic techniques are required to fully understand the effect of the mutation.

If the magnitude of the copper hyperfine coupling and the presence of fewer lines indicates smaller spin density and

only one copper, then there would have to be a vast rearrangement of electron spin density for the His120 mutants. One could postulate that while one copper was losing spin, the other could concurrently gain it in the course of valence localization; the net population of spin on the cysteine sulfur could then conceivably stay constant in the process. However, this explanation would also need to postulate a change of conformation of the remaining histidine (His46) to explain why the nitrogen hyperfine coupling to that nonmutated histidine, which should be located next to the copper with spin to account for hyperfine coupling to ^{14}N of His46, should stay constant. Conversely, if it were to be supposed that the His120 mutants are mixed-valent, then there would need to be a marked change in the Cu hyperfine coupling for one copper, while the spin density throughout the overall CuSSCu site remained unchanged. We are left with a puzzle for the His120 mutants to explain both the constancy of the overall electronic spin distribution implied by ENDOR and the localization of spin on one copper implied by multifrequency EPR. The explanation of the puzzle may require theory at the present state of the art (Gamelin et al., 1998; Neese, 1997), and indeed be a test of that theory, to accurately calculate ligand and metal Fermi and dipolar hyperfine contributions for a Cu_A that explicitly lacks one histidine.

This work was supported by the National Institutes of Health Grant GM-35103 (to C.P.S.) and National Science Foundation CHE95-02421 (to Y.L.). W.E.A. was supported by National Institutes of Health RR01008 to J.S. Hyde. Y.L. also acknowledges the Camille and Henry Dreyfus Foundation for the Camille Dreyfus Teacher-Scholar award. We are grateful to Dr. C.T. Martin, now Prof. of Chemistry, University of Massachusetts, Amherst, for providing the CuLADH sample made in the presence of NADH.

REFERENCES

Antholine, W. E. 1997. Evolution of mononuclear to binuclear Cu_A: an EPR study. *Adv. Biophys. Chem.* 6:217–246.

Atherton, N. M. 1973. Electron Spin Resonance. Wiley, New York.

Beinert, H. 1997. Copper A of cytochrome c oxidase, a novel, long-embattled, biological electron-transfer site. *Eur. J. Biochem.* 245: 521–532.

Berry, S. M., X. Wang, and Y. Lu. 2000. Ligand replacement study at the His 120 site of purple Cu_A azurin. *J. Inorg. Biochem.* 78:89–95.

Blackburn, N. J., M. E. Barr, W. H. Woodruff, J. van der Ooost, and S. de Vries. 1994. Metal-metal bonding in biology: EXAFS evidence for a 2.5 Å copper-copper bond in the Cu_A center of cytochrome oxidase. *Biochemistry.* 33:10401–10407.

Dennison, C., E. Vijgenboom, S. de Vries, J. van der Oost, and G. W. Canters. 1995. Introduction of a Cu_A site into the blue copper protein amicyanin from *Thiobacillus versutus. FEBS Lett.* 365:92–94.

Fan, C., J. Bank, R. Dorr, and C. P. Scholes. 1988. An electron nuclear double resonance (ENDOR) investigation of redox-induced electronic structural change at Cu_A^{++} in cytochrome c oxidase. *J. Am. Chem. Soc.* 263:3588–3591.

Farrar, J. A., P. Lappalainen, W. G. Zumft, M. Saraste, and A. J. Thomson. 1995. Spectroscopic and mutagenesis studies on the Cu_A center from the cytochrome-c oxidase complex of *Paracoccus denitrificans*. *Eur. J. Biochem.* 232:294–303.

Farrar, J. A., F. Neese, P. Lappalainen, P. M. H. Kroneck, M. Saraste, W. G. Zumft, and A. J. Thomson. 1996. The electronic structure of Cu_A: a novel mixed-valence dinuclear copper electron-transfer center. *J. Am. Chem. Soc.* 118:11501–11514.

Froncisz, W., and J. S. Hyde. 1982. The loop-gap resonator: a new microwave lumped circuit ESR sample structure. *J. Magn. Reson.* 47: 515–521.

Froncisz, W., C. P. Scholes, J. S. Hyde, Y. H. Wei, T. E. King, R. W. Shaw, and H. Beiner. 1979. Hyperfine structure resolved by 2 to 4 GHz EPR of cytochrome c oxidase. *J. Biol. Chem.* 254:7482–7484.

Gamelin, D. R., D. W. Randall, M. T. Hay, R. P. Houser, T. C. Mulder, G. W. Canters, S. de Vries, W. B. Tolman, Y. Lu, and E. I. Solomon. 1998. Spectroscopy of mixed-valence Cu_A-type centers: ligand-field control of ground-state properties related to electron transfer. *J. Am. Chem. Soc.* 120:5246–5263.

Greenwood, C., B. C. Hill, D. Barber, D. G. Eglinton, and A. J. Thomson. 1983. The optical properties of Cu_A in bovine cytochrome c oxidase determined by low-temperature magnetic-circular-dichroism spectroscopy. *Biochem. J.* 215:303–316.

Gurbiel, R. J., Y. C. Fann, K. K. Surerus, M. M. Werst, S. M. Musser, P. E. Doan, S. I. Chan, J. A. Fee, and B. M. Hoffman. 1993. Detection of two histidyl ligands to Cu_A of cytochrome oxidase by 35-GHz ENDOR: $^{14,15}N$ and $^{63,65}Cu$ ENDOR studies of the Cu_A site in bovine heart cytochrome aa_3 and cytochromes caa_3 and ba_3 from *Thermus thermophilus. J. Am. Chem. Soc.* 115:10888–10894.

Hay, M., J. H. Richards, and Y. Lu. 1996. Construction and characterization of an azurin analog for the purple copper site in cytochrome c oxidase. *Proc. Natl. Acad. Sci. U.S.A.* 93:461–464.

Hay, M. T., M. C. Ang, D. R. Gamelin, E. I. Solomon, W. E. Antholine, M. Ralle, N. J. Blackburn, P. D. Massey, X. Wang, A. H. Kwon. 1998. Spectroscopic characterization of an engineered purple Cu_A center in azurin. *Inorg. Chem.* 37:191–198.

Hoffman, B. M., V. J. DeRose, P. E. Doan, R. J. Gurbiel, A. L. P. Housman, and J. Telser. 1993. *In* Biological Magnetic Resonance Vol. 13: EMR of Paramagnetic Molecules. L.J. Berliner and J. Reuben, editors. Plenum, New York.

Iwata, S., C. Ostermeier, B. Ludwig, and H. Michel. 1995. Structure at 2.8 Å resolution of cytochrome *c* oxidase from *Paracoccus denitrificans*. *Nature.* 376:660–669.

Karpefors, M., C. E. Slutter, J. A. Fee, R. Aasa, B. Kjellebring, S. Larsson, and T. Vänngård. 1996. Electron paramagnetic resonance studies of the soluble Cu_A protein from the cytochrome *ba3* of *Thermus thermophilus. Biophys. J.* 71:2823–2829.

Kroneck, P. M. H., W. E. Antholine, D. H. W. Kastrau, G. Buse, G. C. M. Steffens, and W. G. Zumft. 1990. Multifrequency EPR evidence for a bimetallic center at the Cu_A site in cytochrome c oxidase. *FEBS Lett.* 268:274–276.

Luchinat, C., A. Soriano, K. Djinovic-Carugo, M. Saraste, B. G. Malmström, and I. Bertini. 1997. Electronic and geometric structure of the Cu_A site studied by ^1H NMR in a soluble domain of cytochrome c oxidase from *Paracoccus denitrificans. J. Am. Chem. Soc.* 119: 11023–11027.

Maki, G., and B. McGarvey. 1958. Electron spin resonance in transition metal chelates: I. Cu(II) bis actetylacetonate. *J. Chem Phys.* 29:31–34.

Maret, W., and H. Kozlowski. 1987. Electronic absorption and EPR spectroscopy of copper alcohol dehydrogenase: pink, violet and green forms of a Type 1 copper center analog. *Biochim. Biophys. Acta.* 912:329–337.

McDowell, C. A., A. Naito, D. L. Sastry, Y. U. Cui, K. Sha, and S. X. Yu. 1989. Ligand ENDOR study of copper (II)-doped L-histidine deuterochloride monodeuterohydrate single crystals at 4.2 K. *J. Mol. Struct.* 195:361–381.

Neese, F. 1997. Electronic structure and spectroscopy of novel copper chromophores in biology. Ph.D. thesis. Universität Konstanz, Germany.

Neese, F., R. Kappl, J. Huttermann, W. G. Zumft, and P. M. H. Kroneck. 1998. Probing the ground state of the purple mixed valence Cu_A center in nitrous oxide reductase: a CW ENDOR (X-band) study of the ^{65}Cu, ^{15}N-histidine labeled enzyme and interpretation of hyperfine couplings by molecular orbital calculations. *J. Biol. Inorg. Chem.* 3:53–67.

Neese, F., W. G. Zumft, W. E. Antholine, and P. M. H. Kroneck. 1996. The purple mixed-valence Cu_A center in nitrous-oxide reductase: EPR of the copper-63-, copper-65-, and both copper-65- and [15_N]histidine-enriched enzyme and a molecular orbital interpretation. *J. Am. Chem. Soc.* 118:8692–8699.

Ramaswamy, S., M. el Ahmad, O. Danielsson, H. Jornvall, and H. Eklund. 1996. Crystal structure of cod liver class I alcohol dehydrogenase: substrate pocket and structurally variable segments. *Protein Sci.* 5:663–671.

Robinson, H., M. C. Ang, Y.-G. Gao, M. T. Hay, Y. Lu, and A. H. J. Wang. 1999. Structural basis of electron transfer modulation in the purple Cu_A center. *Biochemistry.* 38:5677–5683.

Schatz, P. N. 1980. A vibronic coupling model for mixed-valence compounds and its application to real systems. *In* Mixed Valence Compounds. R.D. Brown, editor. D. Reidel, Dordrecht, The Netherlands. 115–150.

Sienkiewicz, A., B. G. Smith, A. Veselov, and C. P. Scholes. 1996. Tunable Q-band resonator for low temperature electron paramagnetic resonance/electron nuclear double resonance measurements. *Rev. Sci. Instrum.* 67:2134–2138.

Slutter, C. E., D. Sanders, P. Wittung, B. G. Malmström, R. Aasa, J. H. Richards, H. B. Gray, and J. A. Fee. 1996. Water-soluble, recombinant Cu_A-domain of the cytochrome *ba3* subunit II from *Thermus thermophilus. Biochemistry.* 35:3387–3395.

Solomon, E. I., M. J. Baldwin, and M. D. Lowery. 1992. Electronic structures of active sites in copper proteins: contributions to reactivity. *Chem. Rev.* 92:521–542.

Stevens, T. H., C. T. Martin, H. Wang, G. W. Brudvig, C. P. Scholes, and S. I. Chan. 1982. The nature of Cu_A in cytochrome *c* oxidase. *J. Biol. Chem.* 257:12106–12113.

Tsukihara, T., H. Aoyama, E. Yamashita, T. Tomizaki, H. Yamaguchi, K. Shinzawa-Itoh, R. Nakashima, R. Yaono, and S. Yoshikawa. 1995. Structures of metal sites of oxidized bovine heart cytochrome c oxidase at 2.8 Å. *Science.* 269:1069–1074.

van Camp, H. L., Y. H. Wei, C. P. Scholes, and T. E. King. 1978. Electron nuclear double resonance of cytochrome oxidase: nitrogen and proton ENDOR from the 'copper' EPR signal. *Biochim. Biophys. Acta.* 537: 238–246.

van der Oost, J., P. Lappalainen, A. Musacchio, A. Warne, L. Lemieux, J. Rumbley, R. B. Gennis, R. Aasa, T. Pascher, B. G. Malmstrom. 1992. Restoration of a lost metal-binding site: construction of two different copper sites into a subunit of the *E. coli* cytochrome o quinol oxidase complex. *Embo J.* 11:3209–3217.

Veselov, A., K. Olesen, A. Sienkiewicz, J. P. Shapleigh, and C. P. Scholes. 1998. Electronic structural information from Q-band ENDOR on the Type 1 and Type 2 copper liganding environment in wild-type and mutant forms of copper-containing nitrite reductase. *Biochemistry.* 37: 6095–6105.

Wang, X., S. M. Berry, Y. Xia, and Y. Lu. 1999. The role of histidine ligands in the structure of purple Cu_A azurin. *J. Am. Chem. Soc.* 121:7449–7450.

Werst, M. M., C. E. Davoust, and B. M. Hoffman. 1991. Ligand spin densities in blue copper proteins by Q-band ^1H and ^{14}N ENDOR spectroscopy. *J. Am. Chem. Soc.* 113:1533–1538.

Williams, P. A., N. J. Blackburn, D. Sanders, H. Bellamy, E. A. Stura, J. A. Fee, and D. E. McRee. 1999. The Cu_A domain of *Thermus thermophilus ba3*-type cytochrome *c* oxidase at 1.6 Å resolution. *Nat. Struct. Biol.* 6:509–516.

Wilmanns, M., P. Lappalainen, M. Kelly, E. Sauer-Eriksson, and M. Saraste. 1995. Crystal structure of the membrane-exposed domain from a respiratory quinol oxidase complex with an engineered dinuclear copper center. *Proc. Natl. Acad. Sci. U. S. A.* 92:11955–11959.

Zumft, W. G., A. Dreusch, S. Lochelt, H. Cuypers, B. Friedrich, and B. Schneider. 1992. Derived amino acid sequences of the nosZ gene (respiratory N_2O reductase) from *Alcaligenes eutrophus*, *Pseudomonas aeruginosa*, and *Pseudomonas stutzeri* reveal potential copper-binding residues: implications for the Cu_A site of N_2O reductase and cytochrome-c oxidase. *Eur. J. Biochem.* 208:31–40.

Zumft, W. G., and P. M. H. Kroneck. 1996. Metal-center assembly of the bacterial multicopper enzyme, nitrous oxide reductase. *Adv. Inorg. Biochem.* 11:193–221.